Supporting Information

Synthesis and Growth Mechanism of Iron Oxide Nanowhiskers

Soubantika Palchoudhury,[1] Wei An,[1] Yaolin Xu,[1] Ying Qin,[2] Zhongtao Zhang,[1] Nitin Chopra,[3] Robert A. Holler,[4] C. Heath Turner,[1] Yuping Bao[1*]*

[1]Chemical and Biological Engineering

[2]Alabama Institute for Manufacturing Excellence

[3]Metallurgical and Materials Engineering and Center for Materials for Information Technology

[4]Central Analytical Facility

The University of Alabama, Tuscaloosa, Alabama, 35487

[*] Corresponding authors: (Y.B.) E-mail: ybao@eng.ua.edu. Phone: (205) 348-9869. Fax: (205) 348-7558. (C.H.T.) E-mail: hturner@eng.ua.edu. Phone: (205) 348-1733. Fax: (205) 348-7558.

1. Experimental details:

Chemicals. All chemicals were commercially available and used without further purification. These include: Fe(III) chloride (98%, anhydrous, Acros Organics), Fe(II) chloride tetrahydrate (99%, Fluka), potassium oleate (40 wt% paste in water), oleic acid (OA, Fischer), tri-n-octylphosphine oxide (TOPO, 90%, Sigma-Aldrich), oleylamine (ON, 70%, Sigma-Aldrich), hexane (99%, Sigma-Aldrich), ethanol (VWR, 99%), 1-octadecene (90%, technical grade, Sigma-Aldrich)

Synthesis of the Fe (III) oleate complex. The iron oleate complex was produced using a published procedure with slight modifications.[1] Briefly, potassium oleate (192.4 g) was mixed with ferric chloride (13 g) in a solvent mixture (hexane, 280 mL and ethanol, 160 mL) at 70 ºC for four hours. The mixture was then phase-separated in a separation funnel. The organic phase containing iron oleate complex was then washed with de-ionized water and dried inside a chemical hood at room temperature. The entire process was performed in air without inert gas protection.

Synthesis of the Fe(II) oleate and Fe (III)/Fe(II) oleate complexes. The Fe(II) oleate and the Fe(III)/Fe(II) oleate complex mixture were prepared to understand the formation mechanism of the nanowhiskers. Specifically, Fe(III) chloride (4.3 g) and Fe(II) chloride (1.69 g, Fe^{3+} /Fe^{2+} = 2:1) or Fe(II) chloride (5.07g) were reacted with the sodium oleate (36.5 g) in a solvent mixture (hexane-140 mL, ethanol-80 mL, and water-60 mL) at 60 ºC for four hours. The mixture was processed in the same way as the Fe(III) oleate complex. However, the entire process was performed under an argon atmosphere to prevent the oxidation of Fe(II).

Electronic structure calculations of the iron oleate complex. The optimal geometric structures of Fe(III) and Fe(II) oleate complexes were predicted with electronic structure

calculations using Gaussian03.[2] The geometric optimization of the complexes was performed using all-electron density-functional theory (DFT) with the popular B3LYP (Becke, three-parameter, Lee-Yang-Parr)[3,4] hybrid exchange-correlation functional and 6-31+G(d) basis set.[5, 6] Diffuse functions were exclusively applied to Fe and O in the carboxyl groups, in which electron lone pairs play a key role in the formation of coordination bonds. The binding energies (BEs) of the first, second, and third ligand of the iron oleate complex were defined as: $BE_1 = [E_{Fe(OA)_3} - (E_{Fe(OA)_2^+} + E_{OA^-})]$, $BE_2 = [E_{Fe(OA)_2^+} - (E_{Fe(OA)_1^{2+}} + E_{OA^-})]$ and $BE_3 = [E_{Fe(OA)_1^{2+}} - (E_{Fe^{3+}} + E_{OA^-})]$, where E is the energy of an isolated species in the gas phase. Hence, negative (positive) BEs denotes an exothermic (endothermic) binding process. An iron oxide nanocluster model, $Fe_{39}O_{62}(HCOO)_{12}$, was built and optimized using the B3LYP functional, with an STO-3G basis set for C, H, and O, and an LANL2DZ effective core potential for Fe. This iron oxide nanocluster has a $(Fe_2O_3)_x$ center with a diameter of 1.1 nm and an oleate ligand shell, where the iron oxide center has a spinel structure with S_6 symmetry, similar to that of maghemite iron oxide nanoparticles.

Thermogravimetric analysis (TGA). TGA measurements were conducted to study the thermal decomposition behavior of Fe(III) oleate, Fe(II)/Fe(III) oleate, and the iron oxide nanowhiskers. Specifically, TGA experiments were performed on a TA Instruments TGA 2950 thermogravimetric analyzer (New Castle, DE) under a nitrogen atmosphere at a constant heating rate of 1 or 5 ^{o}C min^{-1} from room temperature to 500 ^{o}C. The isothermal analysis was conducted by first heating the sample to 80 ºC for 30 min to remove moisture, followed by 3.5 hours of heating at 150 ºC. The use of inert gas protection was important for avoiding any premature oxidation and/or capping ligand combustion.

Synthesis of iron oxide nanowhiskers. Iron oxide nanowhiskers were synthesized by heating the iron oleate complex (1.8 g) in 1-octadecene (13 mL) at 150 ºC in the presence of capping ligands (0.3 mL OA, 0.1 OA mL/0.2 g TOPO, or 0.1 mL OA/0.2 mL ON). The reaction was kept at the reaction temperature for 2.5 hours under an argon atmosphere. Nanoparticle syntheses using Fe(II) oleate, Fe(II)/Fe(III) oleate mixture, Fe(II) stearate, and Fe(III) stearate as precursors were performed under similar conditions using OA only as the capping ligand. The reaction temperature was set at 230 °C for stearate reactions, and 185 °C for Fe(II) oleate reaction, instead 150 °C based on the TGA analysis.

Characterization of iron oxide nanowhiskers. The size, structure, and morphology of iron oxide nanowhiskers were examined on a FEI Technai F-20 TEM. The magnetic properties were studied on a Princeton Alternating Gradient Magnetometer (AGM). Fourier Transform Infrared (FTIR) spectra of the iron oleate complex and the ligand-coated nanowhiskers were collected in order to understand the binding environment. The FTIR studies were performed on a PerkinElmer Spectrum 100 FT-IR spectrometer (Bucks, UK), equipped with an attenuated total reflectance (ATR) cell by accumulation of 4 scans, with a resolution of 2 cm^{-1}. The Fe valance states of the iron oxide nanowhiskers were studied using x-ray photoelectron spectroscopy (XPS) on a Kratos AXIS 165 Multitechnique Electron Spectrometer, equipped with a monochromatic x-ray source (Al, hv = 1486.6 eV). The Raman spectrum of iron oxide nanowhiskers were collected using a Bruker Senterra system (Bruker Optics Inc. Woodlands, TX) equipped with 785 nm laser source at 10 mW laser power and 20X objective.

2. TGA analysis of the iron oleate complex

A TGA measurement were conducted at a constant heating rate of 1 $^{o}C\ min^{-1}$ from room temperature to 500 ^{o}C to compare the heating rate effects on the decomposition process of the

iron oleate complex (Figure S1a). Further, an isothermal analysis was performed by first heating the sample to 80 ºC for 30 min to remove moisture, followed by 3.5 hours of heating at 150 ºC (Figure S1b).

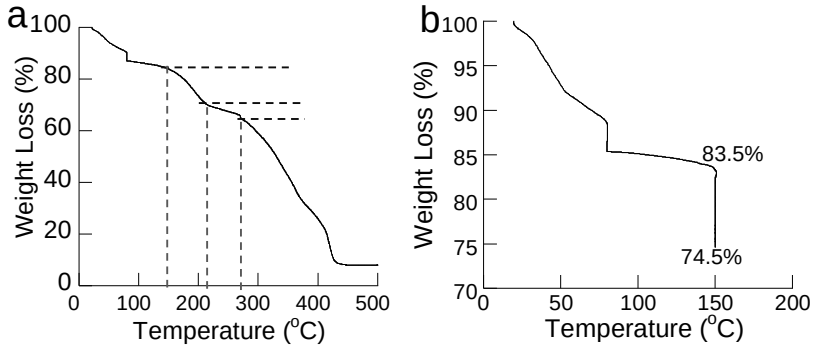

Figure S1. TGA plot of Fe(III) oleate complex (a) at a heating rate of 1 ºC/min, and (b) the isothermal analysis at 150 ºC.

The TGA plot for the slower heating rate demonstrated the same weight loss onset at around 150 ºC, but it continued until 200 ºC, indicating a slow decomposition process of the two weakly-bound ligands. The isothermal analysis performed at 150 ºC reached a constant weight loss of 9% after approximately 2.5 hours, and contiguous weigh loss was not observed, suggesting the remaining ligands are stable at this temperature.

3. XRD scan of iron oxide nanowhiskers

The crystal structure of the nanowhiskers in powder form was studied on a Bruker AXSD8 Advanced x-ray diffractometer (XRD) using a Co source ($K\alpha$, λ =1.79 Å). The x-ray diffraction scan (Figure S2) did not allow us to confirm the crystal phases of these nanowhiskers, magnetite or maghemite, due to the significant size broadening. However, the noticeable peaks at 35.1°,

41.4°, and 50.4° can be indexed as (220), (311), and (400) crystal planes of the iron oxide structures.

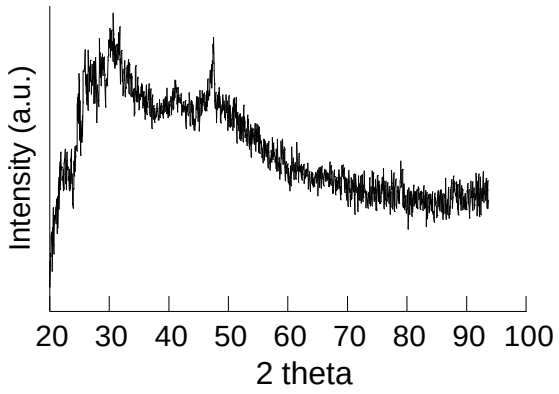

Figure S2. XRD scan of iron oxide nanowhiskers

4. Time-dependent study

To monitor the structural evolution of the iron oxide nanowhiskers, intermediate samples were collected and examined using TEM without any washing. Figure S3 showed the TEM images of samples at reaction time of 1 and 1.5 hours.

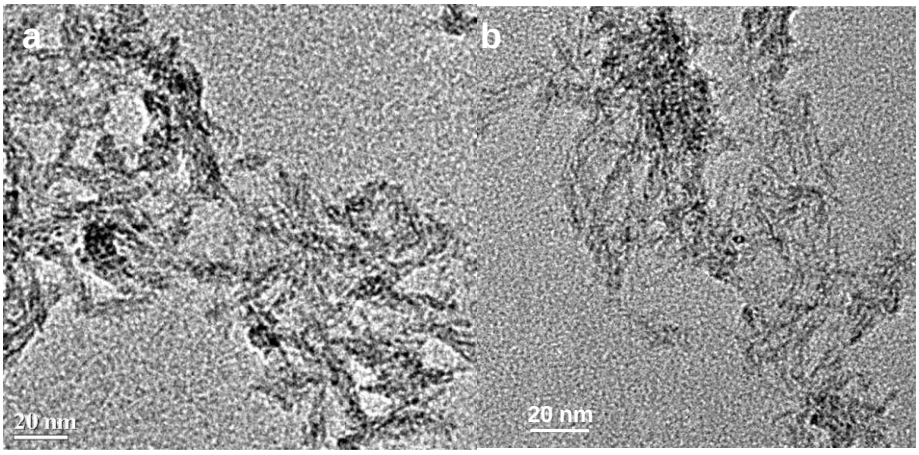

Figure S3. TEM images of intermediate sample at reaction time of (a) 1 hour and (b) 1.5 hours

5. Temperature-dependent study

The TGA measurements and the calculated binding energies of the Fe(III) oleate complex both suggest that the reaction temperature is a critical parameter for the nanowhisker formation. The decomposition of the more weakly-bound ligands was in the range of 150-200 ºC according to the TGA plot. Therefore, reactions were conducted at temperatures below, above, and within this range to investigate the temperature effects on the nanowhisker formation. Reactions at 80, 100, and 120 ºC did not produce whisker-like morphology; instead, dark pasty materials were observed. Figure S4a shows the TEM image of a sample generated at 100 ºC. Reactions performed at 140, 160 and 180 ºC all produced nanowhiskers, similar to the nanowhiskers synthesized at 150 ºC. Figure S4b shows the TEM image of a sample generated at 180 ºC. Interestingly, the reaction performed at 230 ºC produced nanowhiskers with broken pieces, forming small irregular nanoparticles (Figure S4c).

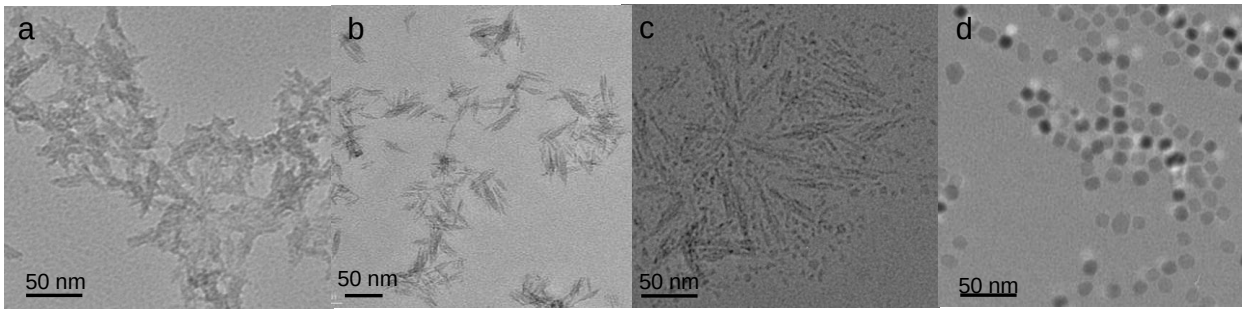

Figure S4. Temperature-dependent nanostructural morphologies: (a) paste-like, 100 ºC, (b) nanowhiskers, 180 °C, (c) irregular nanoparticles, 230 ºC, and (d) nanoparticles, 320 ºC.

This tendency is likely due to the further decomposition of the remaining ligand. Further, spherical nanoparticles were observed for a reaction conducted above 300 ºC, as commonly reported in the literature. Therefore, nanowhisker formation can only be achieved when the

reaction temperature is high enough to dissociate the two more weakly-bound ligands, but low enough to keep the third ligand attached.

6. TGA analysis of Fe(II) oleate and Fe(II)/Fe(III) oleate complex mixture

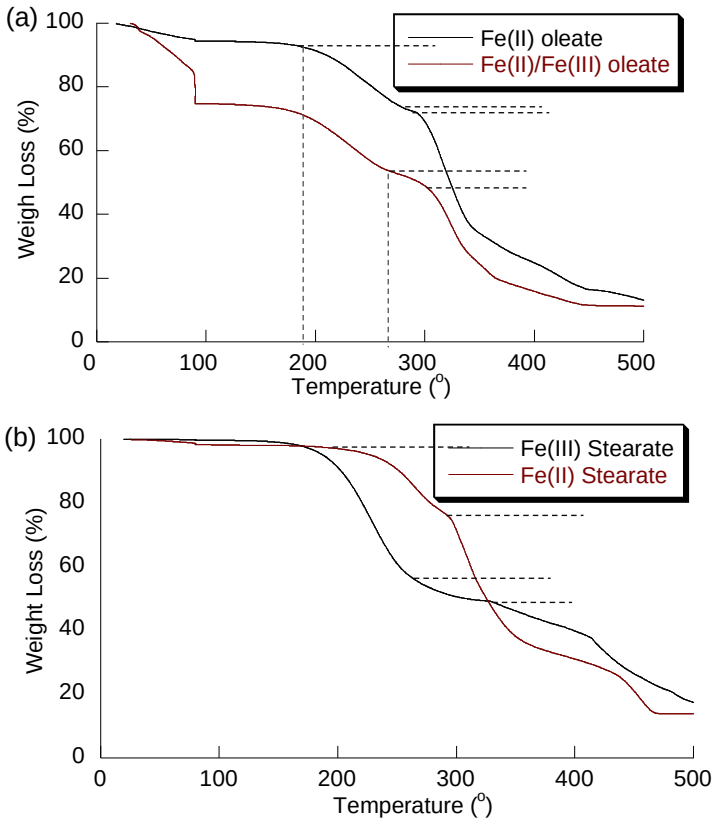

Figure S5. TGA plots of (a) Fe(II) and Fe(II)/Fe(III) oleate complex mixture, and (b) Fe(II) and Fe(III) stearate.

TGA analyses of Fe(II) and Fe(II)/Fe(III) oleate complex mixture at a heating rate of 5 ºC/min were also conducted (Figure S5a). The TGA plot of Fe(II) oleate showed similar weight loss onset to Fe(III) oleate complex, but without evident second weight loss around 230 °C. A very small weight loss region right below 300 °C showed a different rate, which is likely from the possible oxidation of Fe(II) oleate during synthesis or experimental operation. Alternatively, we also performed TGA analyses on commercially available, stable Fe(II) and Fe(III) stearate complexes (Figure S5b, Supporting Information), where the difference in weight losses can be

clearly seen with one weight loss onset for the Fe(II) complex and two for the Fe(III) complex below 300 °C.

7. Effects of alternative ligands

It is well known that selective adsorption of ligands on the nanoparticle crystalline planes can significantly alter the growth pathways of nanoparticles, subsequently leading to the control of nanoparticle geometries.[7] Experiments using surfactant mixtures (OA/TOPO and OA/ON) were performed to investigate the role of alternate ligands on the nanowhisker formation. The obtained nanostructures were then compared with the results from the OA-ligand-only reaction (the normal reaction condition). We have previously reported that TOPO has a weaker binding to iron oxide nanoparticle surfaces than OA, while ON has a stronger binding.[8] The overall ratio of the ligand to the iron precursor was kept the same for all of the reactions.

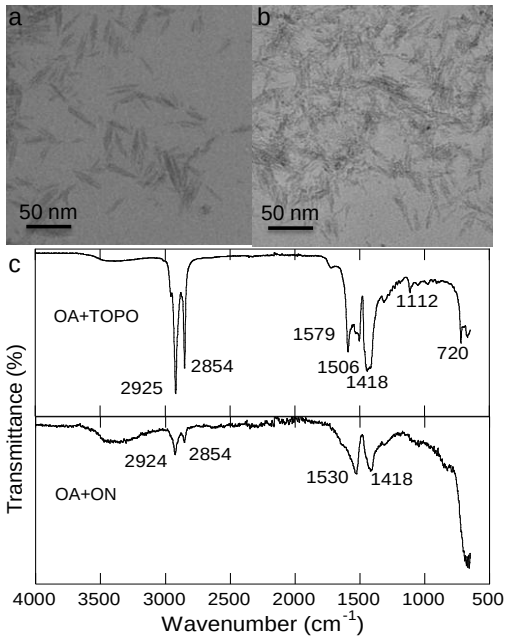

Figure S6. Iron oxide nanowhiskers: (a) synthesized with OA and TOPO, (b) synthesized with OA and ON, and (c) FTIR spectra of these two samples.

Both experiments produced nanoparticles with whisker morphologies (Figure S6a and b). The FTIR spectra of these nanowhiskers did not show detectable signals of TOPO or ON, and the FTIR spectra were similar to the spectrum of the OA-only sample (Figure S6c). The frequency difference between the asymmetrical (ν_{as}) and symmetrical (ν_s) COO^- vibrations for both samples fell within the range of the bridging coordination mode. These observations provide additional evidence that the remaining ligand of the iron oleate complex plays a critical role during the nanostructure formation and that the growth process was not altered by the other ligands.

8. Growth mechanism of iron oxide nanowhiskers

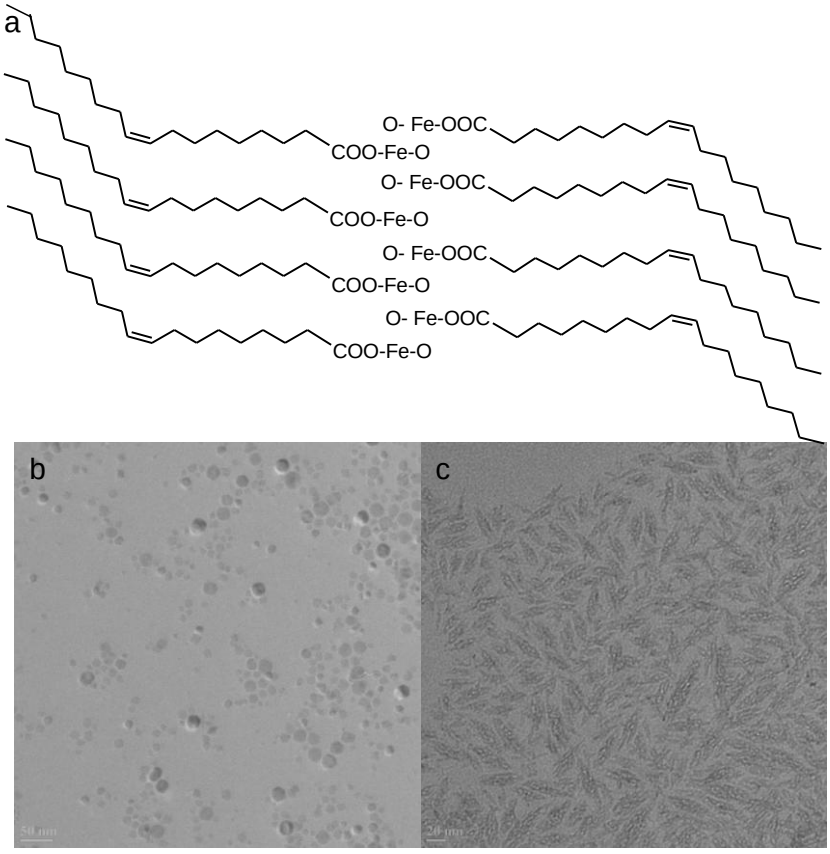

Figure S7. (a) Schematic drawing of the iron oxide nanowhisker formation mechanism, (b) sample produced using Fe(II) stearate at 230 °C, and (c) sample produced using Fe(III) stearate at 230 °C,

We propose that the formation of iron oxide nanowhiskers is a result of remaining ligand interactions, as shown in Figure S7a, where the interaction between the remaining ligands chains played an important role in directing the nanostructure growth. Additionally, to verify our hypothesis, we performed similar reactions at 230 °C using commercially available, stable precursors (*e.g.*, Fe(II) and Fe(III) stearte complexes). Interestingly, very similar results were obtained with the formation of spheres for Fe(II) stearate and 1D nanostructure for Fe(III) stearate (Figure S7 b&c). However, the presence of cavities within the 1D nanostructures need further investigation.

References

1. Park, J.; An, K. J.; Hwang, Y. S.; Park, J. G.; Noh, H. J.; Kim, J. Y.; Park, J. H.; Hwang, N. M.; Hyeon, T. *Nat. Mater.* **2004,** 3, 891-895.

2. M. J. Frisch, e. a. Gaussian 03, Revision E.01, Gaussian, Inc., Wallingford CT,.

3. Lee, C. T.; Yang, W. T.; Parr, R. G. *Phys. Rev. B* **1988,** 37, 785-789.

4. Becke, A. D. *J. Chem. Phys.* **1993,** 98, 5648-5652.

5. Ditchfield, R.; Hehre, W. J.; Pople, J. A. *J. Chem. Phys* **1971,** 54, 5.

6. Rassolov, V. A.; Ratner, M. A.; Pople, J. A.; Redfern, P. C.; Curtiss, L. A. *J. Comput. Chem.* **2001,** 22, 976-984.

7. Hyeon, T. *Chem. Commun.* **2003**, 927-934.

8. Palchoudhury, S.; Xu, Y.; An, W.; Turner, C. H.; Bao, Y. *J. Appl. Phys.* **2010,** 107, 09B311-09B313.